



**HAL**  
open science

# Forcing and evaluating detailed snow cover models with stratigraphy observations

Léo Viallon-Galinier, Pascal Hagenmuller, Matthieu Lafaysse

► **To cite this version:**

Léo Viallon-Galinier, Pascal Hagenmuller, Matthieu Lafaysse. Forcing and evaluating detailed snow cover models with stratigraphy observations. *Cold Regions Science and Technology*, 2020, 180, pp.103163 -. 10.1016/j.coldregions.2020.103163 . hal-03492557

**HAL Id: hal-03492557**

**<https://hal.science/hal-03492557>**

Submitted on 26 Sep 2022

**HAL** is a multi-disciplinary open access archive for the deposit and dissemination of scientific research documents, whether they are published or not. The documents may come from teaching and research institutions in France or abroad, or from public or private research centers.

L'archive ouverte pluridisciplinaire **HAL**, est destinée au dépôt et à la diffusion de documents scientifiques de niveau recherche, publiés ou non, émanant des établissements d'enseignement et de recherche français ou étrangers, des laboratoires publics ou privés.



Distributed under a Creative Commons Attribution - NonCommercial 4.0 International License



# Forcing and evaluating detailed snow cover models with stratigraphy observations

LÉO VIALON-GALINIER<sup>a,b</sup>, Pascal HAGENMULLER<sup>a</sup>, Matthieu LAFAYSSE<sup>a</sup>

<sup>a</sup>Univ. Grenoble Alpes, Université de Toulouse, Météo-France, CNRS, CNRM, Centre d'Études de la Neige, Grenoble, France

<sup>b</sup>École des Ponts, Champs-sur-Marne, France

---

## Abstract

Snow cover models such as Crocus or SNOWPACK have been designed to simulate the detailed stratigraphy of snow properties. This is relevant, for instance, to assess snowpack stability in support of avalanche forecasting. However, such models have generally been evaluated on bulk or surface properties, such as snow depth, water equivalent of snow cover or surface albedo, but not on the detailed stratigraphy. The large number of snow profiles collected in observer networks have thus not been assimilated in such models hitherto. This study introduces a new method to (1) directly compare simulated and observed snow layering and (2) allow for the insertion of observed profile to initialize a snow cover model. This method is mainly based on a scheme to convert observations into state variables of snow cover models and matching observed and simulated layering, accounting for potential depth shifts. The developed methodology was applied to the Crocus snow cover model at three sites in the French Alps, for 15 winter seasons between 2000 and 2015. The performance of Crocus initialized with a bare ground at the end of the summer was evaluated against 739 observed profiles. The model performance varied with the considered winter season and sites. On average, Crocus reproduced snow depth with a median error of 12 cm, layer density with a median error of 50 kg m<sup>-3</sup>, layer grain shape with an error of 0.31 according to a specially developed metric. The re-initialization of the model with observed profiles during winter season enabled to reduce these simulation errors. One week after the direct insertion of a manual profile, the median error of the simulation decreased to 6.8 cm for snow depth, 39 kg m<sup>-3</sup> for density and 0.25 for grain shape. However, the improvement provided by this re-initialization almost completely vanished one month after the insertion.

*Keywords:* snow, snow cover simulation, Crocus, snow stratigraphy, direct insertion

---

## 1. Introduction

Accurately simulating the evolution of the snow cover in time and space is critical for many applications such as climate change assessment, weather forecasting, water resource management, snow management in ski resorts or avalanche hazard forecasting. Depending on the application and desired precision, models of different complexity are used to simulate the snow cover: single-layer snow schemes [e.g. Douville et al., 1995; Bazile et al., 2002], scheme of intermediate complexity [e.g. Loth and Graf, 1998; Boone and Etchevers, 2001] and detailed snow cover models with an explicit representation of the vertical layering [e.g. Vionnet et al., 2012; Bartelt and Lehning, 2002]. These classes of models differ by the vertical resolution, representation of physical properties and parameterizations of physical processes [Vionnet et al., 2012].

10 Snow stratigraphy, i.e. the vertical layering of the snowpack, has long been identified as a major factor for  
11 avalanche formation [Schweizer et al., 2003]. For instance, a pre-requisite for slab avalanche release is the presence of  
12 a weak layer below a more cohesive slab. Avalanche hazard assessment thus requires high-resolution information on  
13 stratigraphy, which can be estimated by detailed snow cover models. Detailed snow models include Crocus originally  
14 developed in France [Brun et al., 1989; Vionnet et al., 2012], SNOWPACK in Switzerland [Bartelt and Lehning, 2002;  
15 Lehning et al., 2002] and SNATHERM in the United States [Jordan, 1991]. Some avalanche forecasting services use these  
16 models in support of their activities and an increasing number of such services intend to use such models [Morin et al.,  
17 2019]. Numerical models provide estimates of the snowpack stratigraphy at a subdaily time resolution (commonly  
18 3 hours) with a more comprehensive spatial coverage than any manual observation. Yet, these estimates can suffer  
19 from large deviations because of errors in the meteorological forcing [Raleigh et al., 2015] and limited accuracy in  
20 simulating complex but essential physical processes such as drifting and blowing snow or liquid water percolation  
21 [Vionnet et al., 2018; D'Amboise et al., 2017; Wever et al., 2014].

22 In addition to the information provided by numerical models, avalanche forecasting services rely on large networks  
23 of observers regularly reporting observed snow profiles [Pahaut and Giraud, 1995]. For instance, about 36,000 profiles  
24 were reported between 1990 and 2015 in French mountains. Manual stratigraphy observations provide a direct snap-  
25 shot of the snowpack at the pit scale, with a specific attention to layers of interest for the assessment of snowpack  
26 stability. However, manual observations are time-consuming and only capture the snowpack evolution at a given time.  
27 Moreover, while these observations provide reliable information on a given point, it is difficult to spatially extrapolate  
28 at a regional scale [Lafaysse et al., 2013; Revuelto et al., 2018].

29 Combining numerical simulations and observed stratigraphy could provide a better representation of snowpack  
30 evolution. However, studies and methods addressing the benefits of jointly using stratigraphy observations and nu-  
31 merical modelling are rather scarce. Only measured meteorological quantities, such as precipitation amount or snow  
32 depth are used to adjust the meteorological forcing or model output. Giraud et al. [2002] developed the computer  
33 program CROCUS\_PC, which simulates the snowpack evolution initialized by a profile fully described in terms of the  
34 Crocus state variables and a time series of meteorological forcing. Snow depth data can be used to drive the model  
35 SNOWPACK [Bartelt and Lehning, 2002]. Charrois et al. [2016] and Larue et al. [2018] showed the potential of assim-  
36 ilating snow surface reflectance into Crocus. Magnusson et al. [2014] introduced a method to assimilate measured  
37 water equivalent of snow cover or bulk snow density. Piazzini et al. [2018] and Smyth et al. [2019] assimilate other  
38 sources of data, such as snow surface temperature or surface albedo. Even if obvious deviations between simulated  
39 and observed profiles are noticed, there is currently no method to correct the snow simulation during the winter season  
40 from detailed observed stratigraphy. This paper introduces a method for direct insertion of observations into snowpack  
41 simulations, as a first step towards more sophisticated assimilation methods.

42 Evaluations of detailed snow cover models have been mostly carried out using bulk or surface properties. For  
43 instance, the model Crocus was evaluated using snow depth [Brun et al., 1989], surface temperature [Brun et al.,  
44 2012], water equivalent of snow cover, bulk snow density or albedo [Lafaysse et al., 2017] but never quantitatively on

45 its detailed simulated stratigraphy. Morin et al. [2013]; Domine et al. [2013] and Carmagnola et al. [2014] compared  
46 observed and simulated profiles of specific surface area but their evaluation remained qualitative. To our knowledge,  
47 Lehning et al. [2001] developed the first method to evaluate simulations of snow stratigraphy, with an illustration on  
48 the model SNOWPACK. To this end, Lehning et al. [2001] used a specific mapping between observed and simulated  
49 layers to account for potential shifts in the layering. The very large set of traditional snowpack observations available  
50 could also be used to evaluate the model, bringing complementary information to classical evaluations, especially on  
51 the detailed stratigraphy [Pahaut and Giraud, 1995; Calonne et al., 2020].

52 This paper introduces a method to evaluate detailed snow cover model output against snow pit observations and to  
53 correct model stratigraphy with these observations. The first pillar of this method is the identification and computation  
54 of common variables between simulation and observation and inferring simulation variables from observations. The  
55 second pillar is a mapping between observed and simulated layers. With these two fundamental pillars, the simulation  
56 can be explicitly evaluated using observed profiles and those can be used to build a new initial model stratigraphy  
57 along the winter season.

## 58 2. Material

59 The data used in this study consists of observed snow profiles describing the snowpack stratigraphy and snowpack  
60 simulations, at three different sites in the French Alps for a 15-year period from 2000 to 2015.

### 61 2.1. Study sites

62 Snowpack observations by trained observers are essential information to estimate avalanche hazard. Therefore,  
63 avalanche warning services maintain extensive networks of observers at dedicated sites [Pahaut and Giraud, 1995]. In  
64 the French mountains, the network of observers operated by Météo-France and its partners in ski resorts is composed  
65 of about 120 observation points at elevations between 1100 m and 3000 m above sea level (Figure 1, for the French  
66 Alps). Around 1300 observed snow profiles are reported each year. For this study, three sites were selected, from  
67 three different massifs, based on their high rate of reporting and low exposure to wind: Col de Porte (Chartreuse,  
68 1325 m, slope 5°, aspect N, [Morin et al., 2012; Lejeune et al., 2019]), Tignes (Haute-Tarentaise, 2400 m, 5°, E) and  
69 La Plagne (Vanoise, 2160 m, 5°, NE). These three sites are highlighted in Figure 1. For the study period and for the  
70 selected sites, 709 complete traditional snow profiles were reported, i.e. about one profile per week during winter.

### 71 2.2. Snowpack observations

72 The snow stratigraphy, i.e. snow physical properties determined layer by layer, is reported in a standardized manner  
73 [Fierz et al., 2009] as follows. Firstly, a measurement of penetration resistance is performed with the ramsonde (ram  
74 measurement not used in this study). Then, after excavating the snowpack down to the ground, the observer divides the  
75 snowpack up to individual homogeneous layers. Each layer is characterized by its vertical position, grain shape and  
76 size, density, hand hardness and wetness according to a standard procedure (see [Fierz et al., 2009] for details). Grain

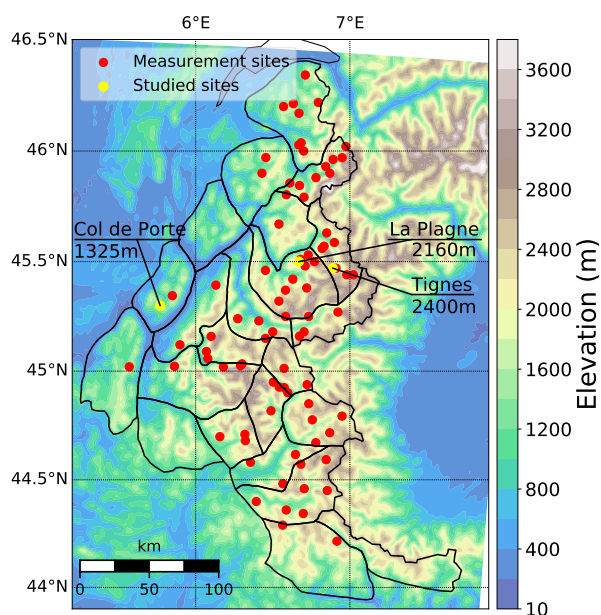


Figure 1. Map of the observer network of Météo-France in the French Alps. The three sites used for this study, namely Col de Porte, Tignes and La Plagne, are highlighted in yellow.

77 shape and size are determined by visual inspection using a crystal card and a magnifying glass (8 x magnification).  
 78 Snow density is measured by weighing a defined snow volume extracted horizontally using a cylinder-type cutter  
 79 (generally 6 cm diameter). Density measurements are usually limited to snow layers thicker than the cutter diameter.  
 80 Hand hardness is measured by pushing the fist (F), four fingers (4F), one finger (1F), a pen (P) or a knife (K) into the  
 81 snowpack. The hand hardness corresponds to the biggest element that can be inserted into snow while not exceeding  
 82 a force of about 10 N. Snow wetness is reported using five classes: dry (D), moist (M), wet (W), very wet (V) and  
 83 soaked (S) according to the snow behaviour if pressed in the glove. In addition to this layer-by-layer observations,  
 84 a temperature profile is measured on an independent vertical grid adjusted by the observer according to temperature  
 85 gradient. In the layer-by-layer characterization, grain shape and layer thickness are always reported but information  
 86 on other characteristics (grain size, hand hardness, wetness and density) can be missing. An example of an observed  
 87 snow profile is shown in Figure 2a.

### 88 2.3. Snowpack simulations

89 The snowpack evolution was simulated using the model SAFRAN-SURFEX/ISBA-Crocus [Durand et al., 1999;  
 90 Lafaysse et al., 2013] at the selected sites.

91 The SAFRAN weather analysis model provides the atmospheric forcing data to drive the snowpack evolution, on  
 92 an hourly basis [Durand et al., 2009]. This model adjusts a guess from numerical weather prediction model at 40 km  
 93 grid spacing using meteorological observation data available (but no snow observations are included). For the French  
 94 Alps, the analysis is performed on 23 areas (so-called massifs) within which the spatial variability of meteorological

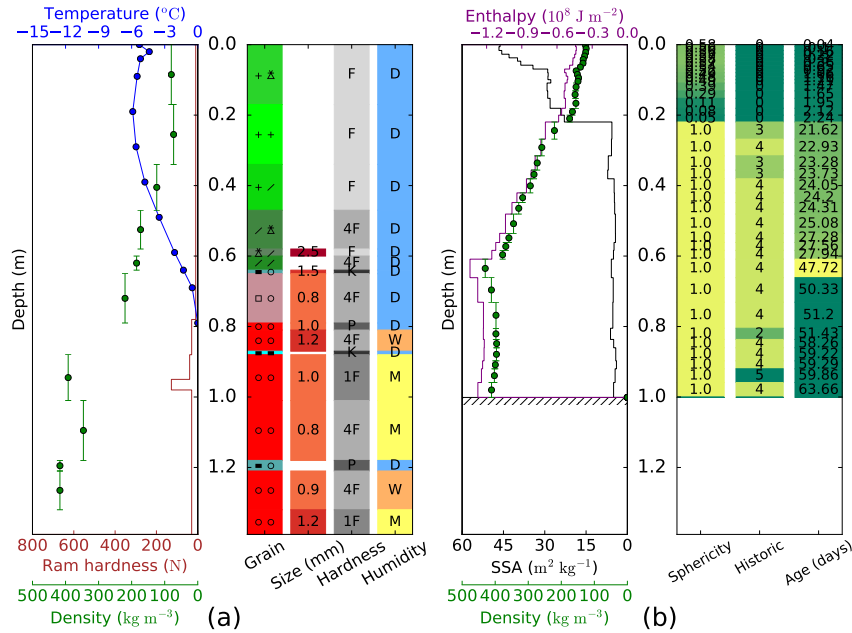


Figure 2. Measured (a) and simulated (b) snow stratigraphy at Col de Porte on February 15th 2005. Grain shape, hand harness and wetness are represented according to the international classification of seasonal snow on the ground [Fierz et al., 2009].

95 and snow conditions are assumed to depend only on elevation, aspect and slope. For the snowpack simulation at the  
 96 sites selected for this study, the atmospheric forcing was interpolated at the exact site elevation and the incoming  
 97 radiation components were adjusted in order to take into account local shading. This large scale meteorological input  
 98 is also used at Col de Porte site, despite the availability of local measurements [Lejeune et al., 2019], for consistency  
 99 with the other sites.

100 The model SURFEX/ISBA-Crocus (referred to as Crocus hereafter) is a one-dimensional multi-layer physical  
 101 snowpack model [Brun et al., 1989; Vionnet et al., 2012]. Crocus represents the snowpack as a set of up to 50  
 102 snow layers. Each layer is characterized by its density, age, enthalpy, mass and two variables representing the snow  
 103 microstructure: sphericity and specific surface area (SSA). An additional state variable, the historic variable, indicates  
 104 whether liquid water or faceted crystals have been present in the layer. SSA represents the total surface area per  
 105 unit of ice mass. Sphericity varies between 0 and 1 and describes the ratio between rounded and angular shapes.  
 106 Crocus reproduces the time-evolution of these state variables by accounting for new snow deposition, metamorphism,  
 107 settlement, heat exchanges, melting and refreezing for each layer, at a time step of 15 minutes. Crocus is coupled to  
 108 the soil scheme ISBA-DIF [Decharme et al., 2011] to account for energy exchanges at the bottom of the snowpack.  
 109 An example of a simulated snow stratigraphy is shown in Figure 2b.

### 110 3. Methods

111 As shown in Figure 2, and described above, the characterization of the snowpack stratigraphy differs between  
112 observations and simulations. In order to evaluate the model or to compute a model initial state from observations,  
113 methods to relate observed and simulated variables as well as to associate observed and simulated layers are required.

#### 114 3.1. Relating simulations and observations

##### 115 3.1.1. Relating observed and simulated snow layer properties

116 The observed layers are described in terms of depth, grain shape and size, density, wetness and hardness. A  
117 temperature profile is also provided, and the temperature profile is assumed to be linear between two measurement  
118 points (Figure 2a). The simulated layers are described in terms of mass, density, SSA, historic variable, sphericity,  
119 enthalpy and age (Figure 2b). To evaluate snow cover model output against observations, simulated variables have to  
120 be converted to observed variables. Conversely, computing an initial model stratigraphy from observations requires a  
121 method to convert observed variables into model state variables.

122 *Using a common set of variables.* The model Crocus already makes it possible to compute layer thickness, density,  
123 grain shape and size, liquid water content and temperature from the simulated state variables [Vionnet et al., 2012].  
124 Layer thickness, density and temperature are common variables of simulations and observations. In contrast, liquid  
125 water content is represented as a continuous variable in the simulation whereas the observer reports a wetness index  
126 between dry and soaked. As the observed class is very subjective, only three classes are retained to compute a common  
127 variable : a class of dry snow corresponding to the observed dry class or to a zero simulated liquid water content, a  
128 class of moist snow corresponding to the observed class moist and simulated liquid water content under  $3 \text{ kg m}^{-3}$ ,  
129 and a saturated class when reported humidity class is wet, very wet or soaked or simulated liquid water content is  
130 above  $3 \text{ kg m}^{-3}$ . Both variables are converted into a three-class variable (dry, moist, saturated) called wetness class  
131 and denoted WetC, according to Appendix A.

132 *Comparing simulated and observed properties.* Comparisons between snow profiles, observed or simulated, are  
133 done on the common set of variables presented in the previous paragraph. The comparison between variables de-  
134 scribed by numerical values, namely snow depth, layer thickness, grain size and temperature is straightforward using  
135 standard metrics such as the deviation (difference between two values) and the error (the absolute value of this dif-  
136 ference). However, a specific metric is required to quantitatively compare grain shapes (categorical variable) and  
137 wetness classes (ordinal variable). To compare grain shapes, we adapted the metric introduced by Lehning et al.  
138 [2001]. We introduced additional grain shapes and consider a distance instead of a score (a distance of 0 means a  
139 perfect agreement). The corresponding distance metric is presented in Table 1. The distance between two mixed grain  
140 shapes  $(p1, s1)$  and  $(p2, s2)$  is defined as  $0.5 \cdot \min(d(p1, p2) + d(s1, s2), d(p1, s2) + d(p2, s1))$ , where  $d$  is the distance  
141 defined in the Table 1 between two "pure" grain shapes. The min function is used so that we do not account for the  
142 order between primary and secondary grain shapes in mixed grain shapes as Crocus does not have such a hierarchical

Grain shape	PP	DF	RG	FC	DH	MF	IF	SH	PPgp
PP	0.0	0.2	0.5	0.8	1.0	1.0	1.0	1.0	0.8
DF	0.2	0.0	0.2	0.6	1.0	1.0	1.0	1.0	0.6
RG	0.5	0.2	0.0	0.6	0.9	1.0	0.0	1.0	0.5
FC	0.8	0.6	0.6	0.0	0.2	1.0	0.0	1.0	0.2
DH	1.0	1.0	0.9	0.2	0.0	1.0	0.0	1.0	0.3
MF	1.0	1.0	1.0	1.0	1.0	0.0	0.2	1.0	1.0
IF	1.0	1.0	0.0	0.0	0.0	0.2	0.0	1.0	1.0
SH	1.0	1.0	1.0	1.0	1.0	1.0	1.0	0.0	1.0
PPgp	0.8	0.6	0.5	0.2	0.3	1.0	1.0	1.0	0.0

Table 1. Distance between two grain shapes, adapted from [Lehning et al., 2001] (with PPgp added with arbitrary values). Snow grain shape abbreviations correspond to the international classification of seasonal snow on the ground [Fierz et al., 2009].

143 way of representing mixed grain shapes (e.g. if the model results indicate DF+FC and the observer reports FC/DF, we  
 144 want to identify this as a perfect agreement as Crocus does not make any difference between DF+FC or FC+DF). To  
 145 compare liquid water classes, an arbitrary value is associated to each class (dry:0, moist:1, saturated:2), which enables  
 146 using standard metrics for the comparison.

### 147 3.1.2. Relating observed and simulated layer boundaries

148 The layer boundaries, i.e. the set of the layer vertical limits, are different between observed and simulated profiles.  
 149 In general, the simulated profile has a much higher resolution and finer structure than the observed profile and layers  
 150 can be shifted vertically between these two profiles. Therefore, it is necessary to perform a mapping between observed  
 151 and simulated layers to obtain a common layer boundary set [Lehning et al., 2001]. The mapping used in this study is  
 152 described below.

153 First, the thickness of the simulated layers is uniformly scaled so that the simulated snow depth corresponds to the  
 154 observed snow depth. The observed and adjusted simulated profiles are then re-sampled on the same vertical layer  
 155 grid of 1 mm (or up to 0.1 mm if some layers are thinner than 1 mm in the simulation) thickness and both expressed  
 156 with common variables (Figure 3a and b). Overall adjustment of layer thicknesses is generally not sufficient to obtain  
 157 a consistent mapping between simulated and observed profiles [Lehning et al., 2001; Hagenmuller and Pilloix, 2016].  
 158 Additional processing is thus required to account for local depth shifts. Following the work of Hagenmuller et al.  
 159 [2018] and Schaller et al. [2016], layer thicknesses are adjusted so that a certain distance  $D$  between the profiles is  
 160 minimized, considering the observed profile as reference. This distance  $D$  is based on the layer metric described in  
 161 detail in Section 3.1.1. It is defined as the mean over depth of the weighted sum of the errors on density ( $d_d$ ), liquid  
 162 water class ( $d_{wc}$ ), grain shape ( $d_g$ ) and depth. Depth is taken into account in  $D$  to limit depth shifts when those do

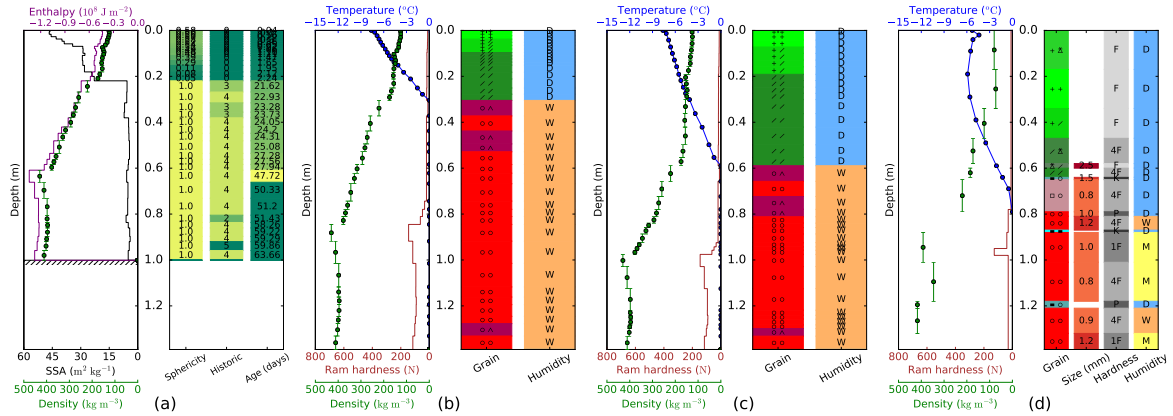


Figure 3. Relationship between the simulated (a, b, c) and observed (d) stratigraphy for 15th February 2005 at Col de Porte. (a) Simulated profile. (b) The simulated snow depth is adjusted and all properties expressed as common variables. (c) Local shifts are adjusted with the matching procedure, so that the stratigraphic features of the simulated profile are at the same depth as the observed profile (d).

not really reduce the general error substantially. Weights are chosen so that each variable equally contribute to  $D$ , accordingly to the following equation:

$$D = \frac{1}{h_{tot}} \int_0^{h_{tot}} \left( \frac{1}{\alpha_d} \cdot d_d + \frac{1}{\alpha_{wc}} \cdot d_{wc} + \frac{1}{\alpha_g} \cdot d_g + \frac{1}{\alpha_h} \cdot |\delta h| \right) dh \quad (1)$$

where  $h$  is the depth,  $h_{tot}$  the snow depth,  $\delta h$  is the depth shift (in m).  $d_d$ ,  $d_{wc}$  and  $d_g$  are defined in Section 3.1.1. Weights are  $\alpha_d = 413 \text{ kg m}^{-3}$ ,  $\alpha_{wc} = 1$ ,  $\alpha_g = 1$  and  $\alpha_h = 1 \text{ m}$ . Note that since the layer properties are often correlated with each other, the layer matching based on  $D$  is not very sensitive to the arbitrary weights chosen in Equation 1. In addition, the layer thickness extension or reduction is constrained to -50% and +100% to avoid very large depth shifts. This constraint prevents very large layer dilation or complete removal of some layers. To solve the optimization problem, i.e. finding the best thickness adjustments according to distance  $D$ , we use Dynamic Time Warping [Sakoe and Chiba, 1978], commonly used in audio or video fields. Dynamic Time Warping finds a global minimum of distance  $D$ , with previously described constraints. Details of this optimization procedure for snow profiles can be found in [Schaller et al., 2016]. An example of the local depth adjustment is shown in Figures 3c, considering the observation of Figure 3d as a reference. In this example, the transition between precipitation and decomposing particles and melt forms of the scaled simulated profile (Figure 3b) was moved from 0.3 m to 0.6 m (Figure 3c) by the matching algorithm to fit the observed profile (Figure 3d).

### 3.2. Evaluation of snow cover models

With the previously described methods, the snowpack simulations can be compared to observed profiles while accounting for potential depth shifts. To this end, the simulation layer boundaries are re-defined so that they match the observed layer boundaries, according to the procedure described in Section 3.1.2. The comparison between

181 simulation and observation is performed at each depth, on the common variables described in Section 3.1.1. Instead  
182 of considering  $D$ , the distance used for the matching (Equation 1), as an overall metric for snow profiles, we rather  
183 present differences between profiles on individual variables (depth, grain shape, density, WetC...). Then, the mean  
184 error is defined as the averaged error on the snow depth. A mean error was also computed on one or several seasons  
185 averaging the error of each comparison point (typically at each observation).

### 186 3.3. Direct insertion of snowpack observations in snowpack simulation

187 In order to generate a model initial state from observed snow profiles, simulation layer boundaries are first mapped  
188 to the observed layer boundaries according to the procedure described in Section 3.1.2. This mapping is necessary to  
189 be able to combine observed and simulated variables.

190 Second, observed variables are converted to model state variables. The relationships between the model state vari-  
191 ables and their observed equivalents, implemented in Crocus, are not directly invertible and additional relationships  
192 were developed. Observed and simulated layer density represent the same physical quantity. Enthalpy is a function of  
193 temperature, liquid water content and density [Boone and Etchevers, 2001, Equation 7]. Liquid water content was es-  
194 timated from wetness class as follows: 0, 2.5 and 5 % of pore volume for dry, moist and saturated classes, respectively.  
195 The snow microstructure variables, namely sphericity, historic variable and SSA, were computed from grain shape  
196 according to the tables shown in Appendix B. Then, the new model initial state is obtained by combining variables  
197 from observations and simulated ones. By default, we used density, enthalpy and grain characteristics (SSA, spheric-  
198 ity and historic) variables computed from observation when available and age from simulation. This set of variable  
199 will be referred to as the basic set. This choice was tested and corresponding results are provided in Section 4.3.3.

200 In the case when there is no snow in the simulated profile but snow in the observed profile with some observed  
201 properties missing (this case appears only once in our data), the new model initial state can not be computed directly.  
202 In this case, a layering compatible with Crocus requirements (maximum 50 layers, thinner layer on top to correctly  
203 solve energy budget, see [Vionnet et al., 2012, sect. 3.2] for details) is produced from observation layering and age  
204 is inferred from grain shape (1 day for precipitation particles as main shape, 6 days for decomposing and fragmented  
205 particles as main shape or precipitation particles as secondary shape and 20 days for other grain shapes).

### 206 3.4. Error metrics

207 The Crocus model is generally driven by meteorological data and initialized with a bare ground in August. In this  
208 case, no snow observation is used. This type of simulation is called hereafter **MMOD**. Evaluating MMOD consists in  
209 comparing the simulated profile to the corresponding observed profile (used as a reference) and computing the error  
210 on each variable as described in Section 3.2. The associated score is hereafter denoted **ERRMOD**.

211 Model simulations corresponding to the direct insertion of observations into the model each time an observation is  
212 available is referred to as **MMIX**. The error of this simulation configuration, considering observations as the reference  
213 is called **ERRMIX**. Each time a direct insertion is performed, we compute the evolution of the snowpack until the end

214 of the season without any further insertion in order to be able to evaluate the persistence over time of the correction.  
215 **ERRMIX** can thus be computed at different time steps after direct insertion: immediately after, i.e. 3 h after insertion,  
216 one week later (1w), typically when the next observation is available, or one month (1m) later, that is four observations  
217 later. This is then denoted **ERRMIX(time since direct insertion)**.

218 To evaluate the interest of direct insertion, **ERRMOD** and **ERRMIX** are compared. For this purpose, the score  
219 **IMPRO(time since direct insertion)** represents the improvement permitted by the direct insertion technique with  
220 respect to the reference run **MMOD**. It is computed as the difference between **ERRMOD**, the reference simulation  
221 error, and **ERRMIX**, the corrected model error:  $\text{IMPRO}(\text{time since direct insertion}) = \text{ERRMOD} - \text{ERRMIX}(\text{time}$   
222  $\text{since direct insertion})$ . To put these errors and improvements in perspective, we compare it to the other data available  
223 for avalanche hazard forecasters, which is the latest previous observation. Using the previous observation as rough ap-  
224 proximation of snowpack actual state is denoted **LOBS** and the error computed with next observation to be compared  
225 to **ERRMOD** is called **ERRLOBS**.

226 These errors can be computed for all common variables, on every subset of the data.

## 227 4. Results

228 The result of our method are first illustrated on one season and one site, before being applied to all the dataset  
229 for quantitative evaluation. In particular, we investigate improvements permitted by the direct insertion, their time  
230 persistence, the interest of direct insertion depending on model error and the influence of the set of variables chosen  
231 for insertion.

### 232 4.1. Example at Col de Porte site

#### 233 4.1.1. Winter season 2003–2004

234 For illustration, we provide results using our method to a single site, Col de Porte, during the winter season  
235 2003–2004 (Figure 4). Here we show only the grain shape and density profiles.

236 Figures 4a and 4d show all snowpack observations available at this site on the considered period (**LOBS**). An  
237 observation is reported approximately every week between mid-December and early April. The observations are here  
238 extended up to the next observation as they are the only data available about the snowpack during this period of time.  
239 As expected, the time persistence of adequacy of an observation, i.e. the duration an observation accurately represents  
240 the snowpack evolving with time, depends on weather conditions. For instance, the snowpack between the 21st and  
241 28th of January evolved rapidly due to snowfall, settlement, dry metamorphism and wet metamorphism. In contrast,  
242 the melt forms and thin ice layers observed on 10th March did not substantially evolve until the next observation on  
243 18th March. This time persistence, estimated as the distance between one observation and the next one, is indeed  
244 variable in time (**ERRLOBS** of 0.64 on grain shape and 0.51 m on snow depth between observations of 21st and 28th  
245 January and 0.42 and 0.47 m, respectively, between 10th and 18th March).

246 Figures 4b and 4e show MMOD simulations. This simulation, called hereafter the reference run, does not exploit  
247 any snowpack observation. The reference simulation exhibits a more continuous layering in time compared to the  
248 observed time series. Grain shape is a categorical variable, so its time evolution inherently presents discontinuities  
249 (jumps from a class to another). Snow depth is substantially underestimated by the simulation during this season by  
250 about 80 cm at the maximum on the 28th January and by 10.5 cm on average for all observations during that winter.  
251 The grain shape profile is reproduced with an error (ERRMOD) of 0.32 to observations. In this test case, Crocus  
252 tends to over-estimate the presence of faceted crystals compared to observations at the beginning of the season and  
253 melt forms mixed with depth hoar at the end where observations mainly indicated melt forms. In addition, Crocus  
254 simulates melt at the snowpack surface in early March, leading to a very high density layer, which is not reported by  
255 any observation.

256 Figures 4c and 4f show the simulated snowpack with the model re-initialized with all observations available  
257 (MMIX). In this case, the simulation is reinitialized every week with a new initial state computed by all observed vari-  
258 ables. The insertion introduces discontinuities in the simulated profiles. However, these discontinuities are smoother  
259 than in the observed time series since Crocus simulates snowpack evolutions, such as the effects of new precipitation  
260 or fast settlement. By re-setting the model snow depth every week, the error on snow depth is, as expected, substan-  
261 tially reduced from an average of more than 35 cm (MMOD) to 0.3 cm (MMIX) immediately after and 5.7 cm one  
262 week after the insertion. The improvement on grain shapes is smaller: the mean error reduces from 0.32 (MMOD)  
263 to 0.14 (MMIX) immediately after and 0.20 one week after. The erroneous simulation of faceted crystals and depth  
264 hoar and the high density layer after an important simulated melting event (see previous paragraph) are corrected by  
265 the direct insertion.

#### 266 4.1.2. Winter seasons 2000–2001 to 2014–2015

267 Here, we report on evaluation results spanning multiple years. The scores of the different snowpack prediction  
268 methods exhibit a high inter-annual variability. Figure 5 shows the evaluation of the different methods on snow  
269 depth, density and grain shape, at Col de Porte for the whole studied period 2000–2015. The three errors ERRLOBS,  
270 ERRMOD and ERRMIX(1w) (the direct insertion is performed one week before the evaluation date) are compared.  
271 For the sake of brevity, only the evaluation on snow depth and density are shown, but the behaviour is the same for  
272 other variables and other sites.

273 During winter 2003–2004, the model exhibits a large deviation from observations in terms of snow depth so that  
274 raw observations from one week before are largely better except during the large snowfall of late January 2004. In  
275 contrast, during winter 2011–2012 the snow depth corresponds better to the observations in the model MMOD and  
276 past observations (LOBS) do not reflect well the current state. Considering only LOBS and MMOD, there is not a  
277 clear signal of which is the better, for these metrics, as model MMOD outperforms in 50.6% of cases for snow depth,  
278 47.6% for density and 40.7% on grain shape on the 231 dates used. However, the corrected model MMIX has lower  
279 deviations in the majority of cases, with regard to observations LOBS (76% on snow depth, 71% on density and 63%

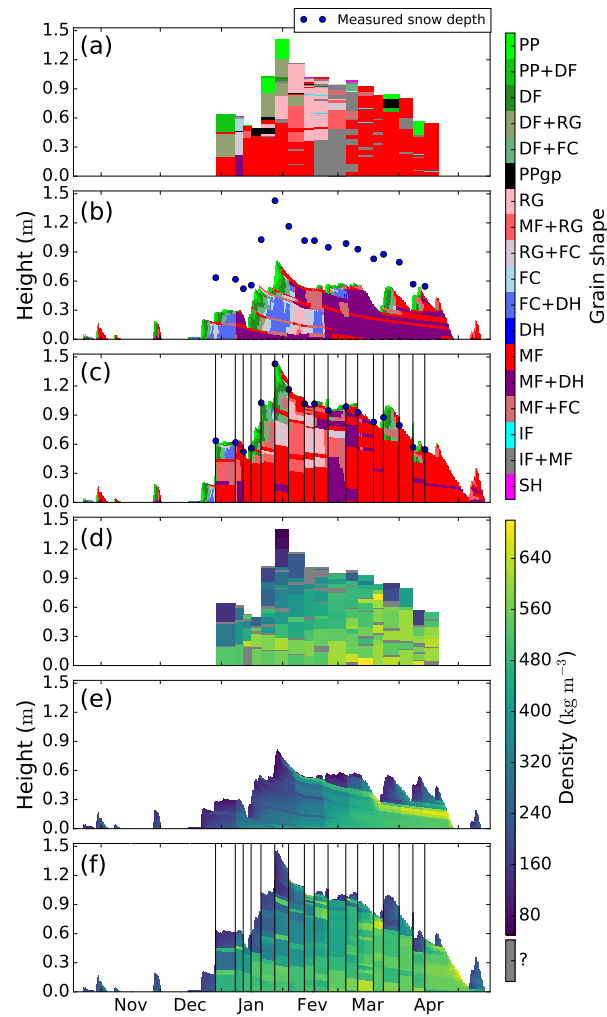


Figure 4. Application on the simulation of the snowpack evolution at Col de Porte during winter season 2003–2004. The subplots (a, b, c) represent the grain shape profiles obtained by different methods, and (d, e, f) the density. (a, d) Measured snow profiles LOBS. (b, e) Reference simulation MMOD. (c, f) MMIX with direct insertion each time an observed profile was available (almost each week). Grey values (referred to as "?") correspond to layers where density values have not been reported.

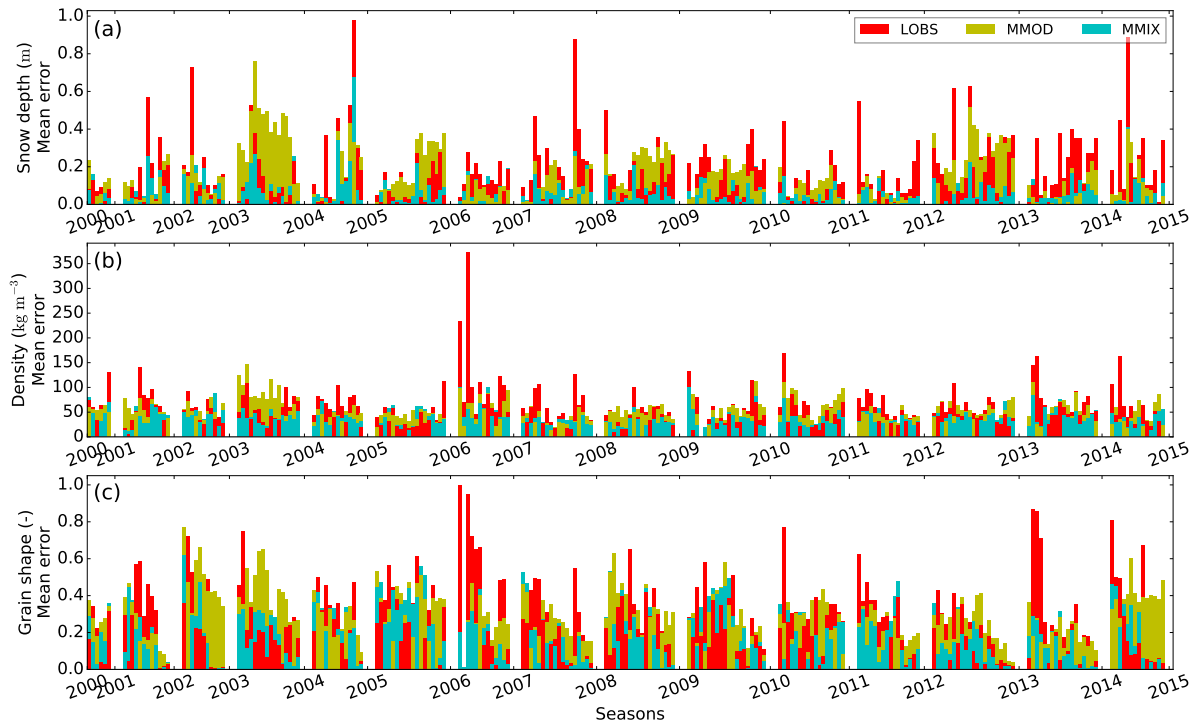


Figure 5. Evaluation of the different snowpack prediction methods at Col de Porte on the period 2000–2015. Top of the bars represent ERRLOBS in red, ERRMOD in green and ERRMIX(1w) in blue. On x-axis are juxtaposed different observations in the chronological order, season by season. Years are labelled between seasons, so observations for winter 2008-2009 are between ticks 2008 and 2009. These errors are plotted here for two variables: (a) snow depth, (b) snow density and (c) grain shape (mean over snowpack depth for density and grain shape).

280 on grain shape) and reference run MMOD (73% on snow depth, 76% on density and 78% for grain shape).

#### 281 4.2. Evaluation of the Model

282 ERRMOD error is presented in Figure 6 for different parameters. The median error on snow depth is around  
 283 12 cm, 50 kg m<sup>-3</sup> on density, 0.3 on grain shape and 0.075 on water class. To put these values in perspective, we  
 284 compare ERRMOD to ERRLOBS, for which median error is around 13 cm on snow depth, 40 kg m<sup>-3</sup> on density,  
 285 0.2 on grain shape and 0.03 on water class. Sometimes, ERRLOBS is much higher than ERRMOD, especially when  
 286 snowfall, rainfall events or strong melting occurs between the previously available observation and the evaluation  
 287 time step. However, on average during the whole season, ERRMOD and ERRLOBS are of the same magnitude. In  
 288 other words, the current snowpack is, in average, as well represented by the previous observation collected one week  
 289 before as by the model initialized with a bare ground in the summer. Over all sites and seasons, the errors using the  
 290 latest previous observation are of the same order of magnitude, quite similar for snow depth and snow density and  
 291 the median error is even lower for grain shape and WetC. To put this analysis in perspective, we need to consider  
 292 that observations are more scarce in early winter and at the end of the season during melting, when the snowpack

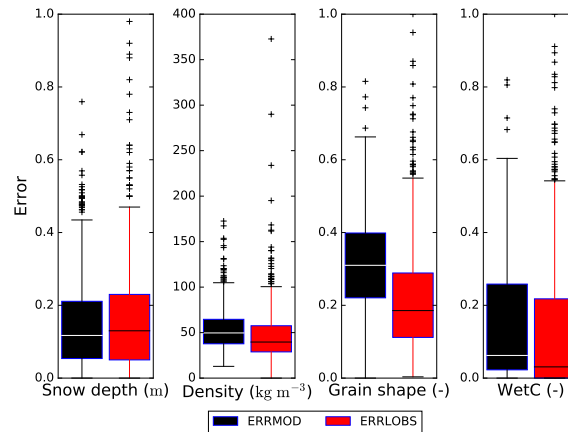


Figure 6. Evaluation of the model (MMOD, in black) error on all sites on the period 2000–2015, compared to the error made using the last available observation (LOBS, in red). The boxes span the inter-quartile range from the 1st to 3rd quartile with the horizontal line showing the median. The whiskers show the range of observed values that fall within 1.5 times the interquartile range and the black crosses are outliers above or below it.

293 experiences its most important evolutions and considering that snow cover models have shown to be relevant when  
 294 major changes occur in the snowpack [Brun et al., 1989, 2012; Lafaysse et al., 2017].

### 295 4.3. Evaluation of direct insertion

#### 296 4.3.1. Time evolution of the improvement allowed by direct insertion

297 To evaluate the impact of direct insertion, ERRMIX is computed at different time steps after insertion (3h, one  
 298 week, one month) and compared to the reference run (ERRMOD), as presented in Figure 7. The error one week after  
 299 insertion gives an idea of the maximum improvement while the error one month after informs on the time persistence  
 300 of potential improvements due to the insertion of observations.

301 The values of ERRMIX(3h) on snow depth, density after insertion are very low compared to ERRMOD, which  
 302 means that the model can be almost perfectly adjusted on these variables. The little difference comes from the time  
 303 between insertion and evaluation of error called immediately after, which corresponds to the output time step of the  
 304 model (three hours). In this period of time, the model simulates settling of the snowpack and melting occurs in the  
 305 snowpack with incoming radiation and heat exchange. In contrast, only partial adjustment of grain shape is possible.  
 306 The difficulty to correct grain shape is partly due to grain shapes which are not coded in Crocus such as ice formations,  
 307 surface hoar and graupel, which represents 27.4% of all observed layers and 11.1% in terms of overall snow layer  
 308 thickness. It is also influenced by error on liquid water content as grains are identified differently by Crocus whether  
 309 the snowpack is dry or not. For WetC, an intermediate level of adjustment is reached after three hours.

310 The impact of a direct insertion into the snow cover model on deviation with observations tends to decrease  
 311 with time. For all considered variables the error is much lower than in reference run immediately after, highlighting  
 312 the interest of correcting the model with observations, but this improvement decreases with time. One month after,

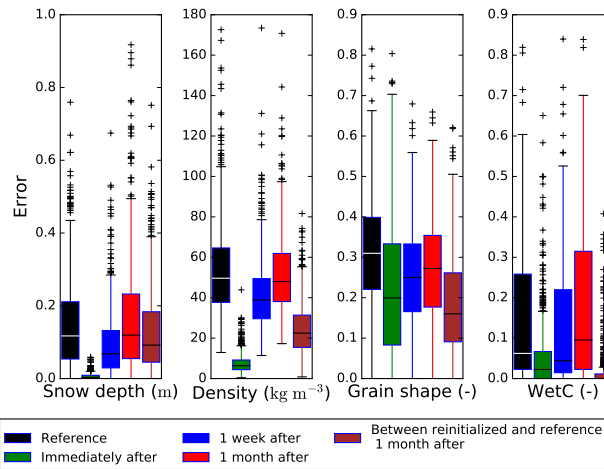


Figure 7. ERRMOD (black) and ERRMIX immediately after the insertion (3 h after, green), one week (next observation, blue) and one month (4th observation after, red) for snow depth, density, grain shape and WetC. The distance between MMIX and MMOD one month after insertion is also shown (brown). Dataset of the three stations and 15 seasons (2000–2015). For box plot definition, see Figure 6.

313 ERRMIX(1m) is close to ERRMOD, and even higher for snow depth and WetC; in other words the improvement of  
 314 direct insertion is lost. Two main differences between the metrics could nevertheless be noted: the initial improvement  
 315 and the evolution rate of error over weeks.

316 The time evolutions of the error values depends on the considered variable. For grain shape, the initial improve-  
 317 ment is limited but it reduces more slowly with time (longer persistence) than for snow depth or WetC. For snow depth,  
 318 even though correction is partially conserved after one week, it is completely lost after one month. Improvement on  
 319 WetC is lost more quickly as there is no substantial improvement on average after one week and the model without  
 320 any correction MMOD exhibits a lower error after one month, which highlights a quick evolution of this variable  
 321 improvement in time.

322 After one month, the direct insertion does not reduce the error of the model. However, this does not mean that after  
 323 one month the MMIX simulation is similar to the reference one (MMOD). To investigate this, the distance between  
 324 MMIX and MMOD after one month is plotted on Figure 7 (brown bars). The behaviour depends on the considered  
 325 variables. For WetC, the MMIX simulated snowpack approaches simulations without insertion. For grain shape and  
 326 density, the state of the MMIX simulated snowpack is closer to the reference run one month after insertion but the  
 327 simulated snowpack remains different from the reference one. In contrast, snow depth of the corrected model is on  
 328 average very different from the reference.

#### 329 4.3.2. Impact of direct insertion as a function of model error

330 In this study, a direct insertion is performed each time an observation is available, including when the model  
 331 state variables are very close to observations. However, direct insertion induces its own uncertainty sources, because  
 332 it does not account for observation errors, and because of filling values for unknown properties (see Section 3.3).

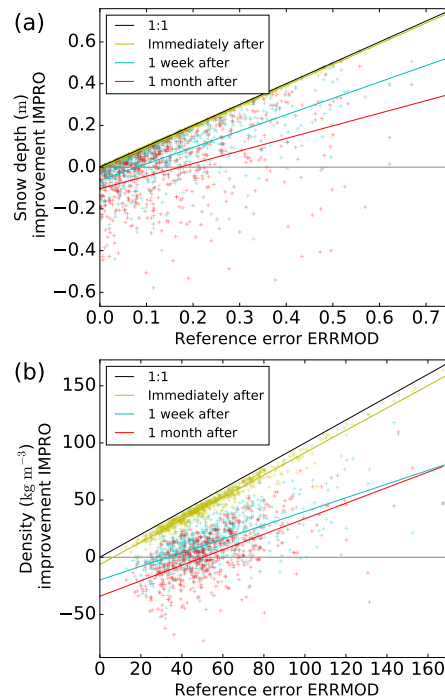


Figure 8. Scatter plot of the improvement IMPRO for different time after insertion depending on ERRMOD at the time of direct insertion. Green crosses represent improvements immediately after (IMPRO(3h)), blue ones refer to one week after (IMPRO(1w)) and red ones refer to one month after (IMPRO(1m)). Solid lines corresponds to linear regressions for each group of symbols. The solid black line represents the maximum improvement (1:1 line). The plot represents (a) snow depth and (b) density. All observations of the dataset considered in this study (3 sites, 15 seasons) are used here.

333 Figure 8 shows an evaluation of the interest of the direct insertion depending on the reference simulation error. The  
 334 improvement indicator IMPRO is plotted immediately after, one week and one month after for two variables: snow  
 335 depth and density. The larger the initial error, the larger the improvement, both one week and one month after. When  
 336 re-initializing with low initial error, the improvement could be low or even highly negative one month after. For  
 337 instance, MMIX reduced deviations with observations ( $IMPRO > 0$ ) in 75% of cases one week after if re-initialized  
 338 for error larger than 2 cm on snow depth and  $130 \text{ kg m}^{-3}$  for density.

#### 339 4.3.3. Selection of variables for direct insertion

340 For all previous results, all state variables of the model were inferred from observation, except age inferred from  
 341 simulation, that is to say density, sphericity, historic variable, SSA and enthalpy, called basic set. The influence of  
 342 each variable has been studied on the mean error on liquid water class, grain shape, density, snow depth, immediately  
 343 after and one week after as shown in Figure 9. Insertion of SSA and density have not much cross impact on other  
 344 variables: errors on other variables are not substantially modified. On the contrary, enthalpy has a wider impact, as it  
 345 determines whether dry or wet metamorphism can take place. We also evaluated the result of using only snow depth

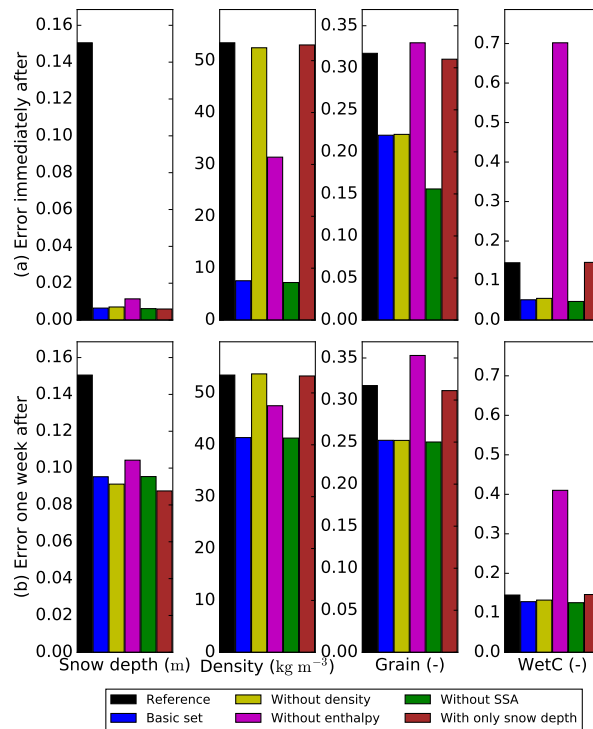


Figure 9. Mean ERRMIX error for a set of variables, immediately after insertion and one week after for different set of inserted variables: in black, nothing inserted (ERRMOD), in blue our basic set chosen (density, sphericity, historic, SSA and enthalpy), in yellow the basic set without density, in pink without enthalpy, in green without SSA and in dark red, with only snow depth and adjusting layer boundaries (thickness). Data generated from averaging absolute errors on seasons 2000 to 2015 on the three stations.

346 (and matching of layer boundaries) for correcting model results. This insertion corrects successfully the snow depth,  
 347 even better than with other variables after one week, but does not substantially improve the other variables considered.

## 348 5. Discussion and conclusion

349 Detailed snow cover models are commonly evaluated on surface or bulk variables, whereas they are designed to  
 350 represent the detailed stratigraphy. Moreover, models used in support to operational avalanche hazard forecasting are  
 351 commonly driven with meteorological data without use of snowpack observations during a whole season, so errors  
 352 accumulate and the simulation increasingly deviates from observations. We contribute in this paper to reduce these two  
 353 limitations. A method for evaluating detailed snow cover models with respect to snow pit observations is introduced  
 354 and direct insertion of observations into snowpack modelling is implemented and used to analyze some key features  
 355 of snow cover dynamics.

### 356 5.1. Model evaluation

357 The evaluation procedure presented in this study provides a fully automated, flexible and reproducible way to  
358 evaluate snow cover model results, and it is complementary to evaluations generally conducted on bulk or surface  
359 variables. Potential depth shifts between observed and simulated snow profiles are corrected with the developed  
360 matching algorithm (Figure 3). In particular, the matching allows to decompose differences between snow profiles  
361 into differences in layer position and differences in layer properties. We did not provide an overall agreement score  
362 as proposed by Lehning et al. [2001], but we decompose the snow cover evaluation on a set of physical and tangible  
363 variables, shared between simulated and observed data, such as snow depth, density, grain shape and wetness classes  
364 (Figure 6).

365 We applied this evaluation to the snow cover model Crocus and conventional snow measurements from three sites  
366 in the French Alps, on seasons from 2000–2001 to 2014–2015. The model performance varied with the considered  
367 winter season and sites (Figure 5). On average, Crocus reproduced snow depth with a median error of 12 cm, layer  
368 density with an error of  $50 \text{ kg m}^{-3}$ , layer grain shape with an error of 0.31 according to a previously developed heuristic  
369 metric and wetness classes with an error of 0.075 (Figure 6). It remains difficult to evaluate whether these levels of  
370 agreement between Crocus and observations can be considered as bad, fair or good. Firstly, this qualitative evaluation  
371 will depend on the considered application [Fierz et al., 2014]. For instance, the assessment of the avalanche danger  
372 and the snowpack mechanical stability will strongly depend on the ability of the snow cover model to accurately  
373 simulate the grain shape (e.g. depth hoar and faceted crystals). For hydrology and predicting run-off, simulating the  
374 grain shape will not be critical but accurately simulating the wetness of the snowpack will be important. Secondly,  
375 these scores have to be put in perspectives with the limited sources of information on the snowpack available. We  
376 showed that the current snowpack is, on average, as well represented by the previous observation collected one week  
377 before as by the model initialized with a bare ground in the summer (Figure 6). Nevertheless, the model remains the  
378 only forecasting method. Besides, the quantitative evaluation of Crocus highlighted some strengths and weaknesses  
379 of the model. Snow depth tended to be better represented by the reference run (Crocus initialized in August) than  
380 the previously available manual observation (Figure 6), consistently with the known ability of Crocus to correctly  
381 simulate snow depth [Revuelto et al., 2018; Vionnet et al., 2019]. In contrast, the liquid water content was better  
382 represented by the previous observation compared to the reference run (MMOD) (Figure 6). The low performance  
383 of the model on liquid water content is consistent with known shortcomings of snow cover models to represent the  
384 complex process of liquid water infiltration with simple bucket schemes [Lafaysse et al., 2017].

### 385 5.2. Direct insertion

386 We showed that direct insertion of snow observations enables to correct snow cover simulations. The improve-  
387 ments provided by the insertion depended on the time between the insertion and the evaluation. Its typical time  
388 persistence was around one week. A perfect agreement between the model and the observation could not be reached  
389 immediately after insertion (Figure 7). This discrepancy was partly due to the absence of some grain shapes in Crocus

390 code and the fact that some observed profiles are not numerically stable according to Crocus empirical parameteriza-  
391 tions. On the considered sites and time period, the median error of the simulation decreased to 6.8 cm for snow depth,  
392  $39 \text{ kg m}^{-3}$  for density and 0.25 for grain shape, one week after the direct insertion of a full manual profile (Figure 7).  
393 In general, the improvement almost vanished one month after the insertion (Figure 7) but remained positive when the  
394 model error was large enough before the insertion (Figure 8).

395 This ineffective correction beyond one month might be due to different sources of errors. Firstly, erroneous  
396 meteorological forcing is known to be an important source of error [Raleigh et al., 2015], especially because the spatial  
397 scale of meteorological analysis (about  $1\,000 \text{ km}^2$ ) cannot represent the local meteorology and because of the scarcity  
398 and uncertainties of assimilated observations. Secondly, many processes in snowpack modelling are represented by  
399 uncertain empirical parameterizations [Lafaysse et al., 2017]. Due to the impossibility to observe independently each  
400 individual process, these parameterizations are only constrained by the commonly available observations such as snow  
401 depth or water equivalent of snow cover. However, different sets of parameterizations lead to similar overall skill of the  
402 model on these data due to error compensation between parameterizations [Lafaysse et al., 2017; Essery et al., 2013;  
403 Krinner et al., 2018]. For instance, the choice of an optimal parameterization for snow compaction highly depends  
404 on the choice of the parameterization of the density of falling snow. In our case, it is known that the parameterization  
405 of falling snow overestimates the observed density [Helfricht et al., 2018] because it compensates the absence of an  
406 explicit dependence of the compaction velocity on snow microstructure. Therefore, adjusting the simulated density  
407 with measured density profile immediately after a snowfall event can highly degrade the score of the model as the  
408 weeks goes by (Figure 7) because of the parameterization of compaction. The error observed on WetC in Figure 7  
409 could also be explained by erroneous water retention and percolation in the snowpack. Last, observations were here  
410 considered as the reference of the snowpack state in this study. Most of these observations are inevitably prone to  
411 errors: even density measurements carry uncertainties [Proksch et al., 2016]. This uncertainty is increased because  
412 different observers are involved, introducing another source of variability for some variables. Moreover, at the study  
413 plot scale (typically 10 m), spatial variability is unavoidable [Harper and Bradford, 2003], even if the plots used for  
414 this study were selected based on their low exposure to wind. Note also that observation errors are not only a limitation  
415 for the efficiency of direct insertion but also for the relevance of model evaluation without insertion.

416 The variables used for the direct insertion were chosen on the basis of available information from conventional  
417 snowpack observations. In general, we used all data available from these observations to re-initialize the model. We  
418 showed that this could be adapted to data available, even with more simple observations which are easier to collect. We  
419 evaluated the impact of the choice of the inserted property on the simulation improvements (Figure 9). For instance,  
420 using only snow depth with adjusted layer boundaries (thickness) enabled to reduce the simulation error one week  
421 after the insertion, but mainly on the snow depth, with a limited cross impact on the other properties (Figure 9).

### 422 5.3. Outlooks

423 The operational modelling system in French mountains areas used by avalanche forecasters is based on the MMOD  
424 configuration, that is to say the simulation of the snowpack is only driven during the whole season by a meteorolog-  
425 ical forcing which only assimilates meteorological observations but no snowpack observations. Errors on snow-rain  
426 elevation limit, snowfall amount or wetting can impact these snowpack simulations during the season. For instance,  
427 we showed that the model chain did not provide substantially better results than using the latest available observation.  
428 However, model performance was variable in time and space. Forecasters using the model should first have to evaluate  
429 the relevance of the model for the planned application before using the simulated snowpack in their analysis. Cur-  
430 rently, there is no existing tool for that purpose. In this context, real-time evaluations of the model, with the presented  
431 metrics, on locations where observations are available, could provide relevant information to the forecaster about the  
432 relevance of the model for the current specific situation. Such real-time evaluations are already performed for Crocus  
433 model on snow depth, but not on any stratigraphic feature.

434 When large errors are noticed, the direct insertion method could reduce errors by re-initializing the snowpack to  
435 a more realistic state and prevent from maintaining large systematic errors for the rest of the season. Even if these  
436 observations only represent the point where they are performed and could hardly be spatialized, modelling snowpack  
437 evolution on these points with a smaller error, or at least limited to a known magnitude, remains interesting. Indeed,  
438 the snow cover model provides an interpolator between observations, with smaller errors compared to a free simulation  
439 — note that this was the initial intent driving the original development of the Crocus snow cover model [Morin et al.,  
440 2019].

441 The evaluation and direct insertion methods are here applied to the Crocus model and conventional snow observa-  
442 tions conducted in a snow pit. However, this method is highly modular and could be straightforwardly adapted to other  
443 detailed snow cover models or other snow observations. In particular, more detailed observations could also be used,  
444 as SnowMicroPen (SMP [Hagenmuller et al., 2016; Pielmeier and Schneebeli, 2003]) data or SSA profiles [Arnaud  
445 et al., 2011], as the ones conducted on a daily to weekly basis at some sites [e.g. Calonne et al., 2020]. Moreover,  
446 the evaluation method could be used to compare and evaluate the stratigraphies simulated by different snow cover  
447 models. Similarly to Krinner et al. [2018], intercomparison and evaluations of detailed snow cover models could also  
448 include an evaluation on the detailed stratigraphy based on an extensive set of conventional snowpack measurements.  
449 In addition, different parameterizations of the same model, such as Lafaysse et al. [2017], could be evaluated in order  
450 to improve snow cover models based on quantitative appraisal of the deviations of model results to observations and  
451 to guide future development efforts.

452 A method to quantify errors between model and observations was developed. The direct insertion of observations  
453 improved most often the simulations, with fluctuations depending on amplitude of model error and availability of  
454 observations. Our method only injects observations in the model by direct insertion, forgetting most of the simulation  
455 results and ignoring observation errors or uncertainties. For instance, injecting an observation when the model error is  
456 very low induced a degradation of the model scores (Figure 8). Direct insertion, a very simple assimilation technique,

457 does not either take into account model uncertainty. Furthermore, the method, as presented, can only be implemented  
458 on points where observations are performed. More advanced assimilation methods such as using ensemble algorithms  
459 [Magnusson et al., 2014; Charrois et al., 2016] are known to be able to solve these limitations of direct insertion.  
460 However, they have only been applied to the assimilation of bulk or surface properties of the snowpack [Helmert  
461 et al., 2018; Langeron et al., 2020]. Our work is a first step towards the possibility to assimilate observed profiles with  
462 such algorithms because it provides a distance metric between observed and simulated profiles. Nevertheless, the use  
463 of this method in spatialized simulations remains difficult due to the lack of observations. In spatialized simulations,  
464 the assimilation of satellite observations of surface properties might be more straightforward [Cluzet et al., 2019] but  
465 they do not provide all the modelled variables, so the use of snow pit observations could be complementary to the  
466 assimilation of remote sensing data.

## 467 **6. Acknowledgements**

468 Authors thank observers of the Météo-France network for reporting almost weekly observations, especially ob-  
469 servers of La Plagne and Tignes ski resorts. We gratefully acknowledge S. Morin for discussions and constructive  
470 comments. We also thank people of CNRM/CEN for collecting data at Col de Porte and for collecting and archiving  
471 all snowpack observations. CNRM/CEN is part of Labex OSUG@2020 (Investissements d’Avenir, grant agreement  
472 ANR-10-LABX-0056). We thank C. Fierz and A. van Herwijnen for their useful comments and suggestions.

## 473 **7. Data and code availability**

474 Crocus is an open-source model available at [https://opensource.umr-cnrm.fr/projects/snowtools\\_](https://opensource.umr-cnrm.fr/projects/snowtools_git/wiki/Procedure_for_new_users)  
475 [git/wiki/Procedure\\_for\\_new\\_users](https://opensource.umr-cnrm.fr/projects/snowtools_git/wiki/Procedure_for_new_users) (version used is referenced as `s2m_reanalysis_2019`). The model con-  
476 figuration is the standard one presented in Lafaysse et al. [2017] (blue cells in Figure 2). Observation data from  
477 Col de Porte have been published by Lejeune et al. [2019]. Other processed data are available upon request to the  
478 corresponding author.

## 479 **Appendix A. Wetness class definition**

480 Liquid water content is represented as a continuous variable in the simulation whereas the observer reports a  
481 wetness class between dry and soaked. These variables have to be cast to a common format before comparison.  
482 As the observed class is very subjective, only three classes are retained to compute a common variable: a class of  
483 dry snow corresponding to the observed dry class or to a zero simulated liquid water content, a class of moist snow  
484 corresponding to the observed index moist and simulated liquid water content under  $20 \text{ kg m}^{-3}$  (equivalent to 2%  
485 in volume), and a saturated class when reported wetness index is wet, very wet or soaked or simulated liquid water  
486 content is above  $20 \text{ kg m}^{-3}$ . This common variable is called wetness class and denoted as `WetC`.

## 487 Appendix B. Completion tables

488 Direct insertion needs to reconstruct model variables from observation. Relations between observed variables  
 489 and model state variables, implemented in Crocus, are not directly invertible and additional relations were therefore  
 490 defined, especially for variables describing grain morphology, namely sphericity, SSA and historic variable. Table B.1  
 491 proposes relations between grain shape identified by the observer and simulation variables. These relations have been  
 492 determined from identification of grain shape in Crocus code [Vionnet et al., 2012] for sphericity and historic, picking  
 493 values in the range of sphericity and historic variable for each grain shape. For SSA, as Crocus has only three classes  
 494 of SSA, the values are chosen to be consistent with Crocus classes but in these classes, values for each grain shape are  
 495 ordered according to measurements of SSA at Col de Porte by Carmagnola [2013] and Domine et al. [2007].

496 Some variables may not have been reported for all layers in an observed profile, especially snow density, which  
 497 could not be measured for thinner layers. To ensure the consistency of the re-initialized state, missing densities are  
 498 filled, based on grain shape reported, with Table B.2. These densities are chosen to be compatible with Crocus grain  
 499 identification.

## 500 References

- 501 Arnaud, L., Picard, G., Champollion, N., Domine, F., Gallet, J., Lefebvre, E., Fily, M., Barnola, J., 2011. Measurement of vertical profiles of snow  
 502 specific surface area with a 1 cm resolution using infrared reflectance: instrument description and validation. *Journal of Glaciology* 57, 17–29.
- 503 Bartelt, P., Lehning, M., 2002. A physical snowpack model for the swiss avalanche warning. *Cold Regions Science and Technology* 35, 123–145.  
 504 doi:10.1016/S0165-232X(02)00074-5.
- 505 Bazile, E., El Haiti, M., Bogatchev, A., Spiridonov, V., 2002. Improvement of the snow parametrisation in arpege/aladin, in: *Proceedings of*  
 506 *SRNWP/HIRLAM Workshop on surface processes, turbulence and mountain effects, Madrid*. pp. 14–19.
- 507 Boone, A., Etchevers, P., 2001. An intercomparison of three snow schemes of varying complexity coupled to the same land surface model: Local-  
 508 scale evaluation at an alpine site. *Journal of Hydrometeorology* 2, 374–394. doi:10.1175/1525-7541(2001)002<0374:AI0TSS>2.0.CO;2.
- 509 Brun, E., Martin, E., Simon, V., Gendre, C., Coleou, C., 1989. An energy and mass model of snow cover suitable for operational avalanche  
 510 forecasting. *Journal of glaciology* 35, 333–342.
- 511 Brun, E., Vionnet, V., Morin, S., Boone, A., Martin, E., Faroux, S., LeMoigne, P., Willemet, J.M., 2012. Le modèle de manteau neigeux crocus et  
 512 ses applications. *La Météorologie* 76, 44–54.
- 513 Calonne, N., Richter, B., Löwe, H., Cetti, C., ter Schure, J., Van Herwijnen, A., Fierz, C., Jaggi, M., Schneebeli, M., 2020. The rhossa campaign:  
 514 multi-resolution monitoring of the seasonal evolution of the structure and mechanical stability of an alpine snowpack. *The Cryosphere* 14,  
 515 1829–1848. URL: <https://tc.copernicus.org/articles/14/1829/2020/>, doi:10.5194/tc-14-1829-2020.
- 516 Carmagnola, C., 2013. *Mesure, analyse et modélisation des processus physiques du manteau neigeux sec*. Ph.D. thesis. Université de Grenoble.
- 517 Carmagnola, C., Morin, S., Lafaysse, M., Domine, F., Lesaffre, B., Lejeune, Y., Picard, G., Arnaud, L., 2014. Implementation and evaluation of  
 518 prognostic representations of the optical diameter of snow in the surfex/isba-crocus detailed snowpack model. *The Cryosphere* 8, 417–437.
- 519 Charrois, L., Cosme, E., Dumont, M., Lafaysse, M., Morin, S., Libois, Q., Picard, G., 2016. On the assimilation of optical reflectances and snow  
 520 depth observations into a detailed snowpack model. *The Cryosphere* 10, 1021–1038. doi:10.5194/tc-10-1021-2016.
- 521 Cluzet, B., Revuelto, J., Lafaysse, M., Tuzet, F., Cosme, E., Picard, G., Arnaud, L., Dumont, M., 2019. Towards the assimilation of satellite  
 522 reflectance into semi-distributed ensemble snowpack simulations. *Cold Regions Science and Technology* , 102918doi:[https://doi.org/10.](https://doi.org/10.1016/j.coldregions.2019.102918)  
 523 [1016/j.coldregions.2019.102918](https://doi.org/10.1016/j.coldregions.2019.102918).

(a) Sphericity									
Secondary grain	PP	DF	RG	FC	DH	MF	IF	SH	PPgp
Main grain									
PP	0.50	0.50	0.75	0.25	0.00	0.99	0.50	0.50	0.45
DF	0.50	0.50	0.70	0.30	0.00	0.99	0.50	0.50	0.45
RG	0.90	0.80	0.99	0.60	0.50	0.99	0.99	0.90	0.75
FC	0.10	0.20	0.40	0.00	0.00	0.30	0.30	0.00	0.10
DH	0.00	0.00	0.60	0.00	0.00	0.50	0.25	0.00	0.50
MF	0.99	0.99	0.99	0.45	0.70	0.99	0.99	0.90	0.90
IF	0.50	0.50	0.99	0.30	0.25	0.99	0.50	0.50	0.50
SH	0.50	0.50	0.90	0.50	0.50	0.90	0.50	0.50	0.50
PPgp	0.45	0.45	0.65	0.10	0.50	0.75	0.50	0.50	0.50

(b) Historic variable									
Secondary grain	PP	DF	RG	FC	DH	MF	IF	SH	PPgp
Main grain									
PP	0 (2)	0 (2)	0 (2)	0 (3)	1 (3)	2 (2)	2 (2)	1 (3)	0 (2)
DF	0 (2)	0 (2)	0 (2)	1 (3)	1 (3)	2 (2)	2 (2)	1 (3)	0 (2)
RG	0 (2)	0 (2)	0 (0)	0 (0)	1 (3)	2 (2)	2 (2)	1 (3)	0 (2)
FC	1 (3)	1 (3)	0 (0)	0 (0)	1 (3)	3 (3)	3 (3)	1 (3)	1 (3)
DH	1 (3)	1 (3)	1 (3)	1 (3)	1 (1)	3 (3)	3 (3)	1 (3)	1 (3)
MF	2 (2)	2 (2)	2 (2)	3 (3)	3 (3)	2 (2)	2 (2)	3 (3)	2 (2)
IF	3 (3)	3 (3)	3 (3)	3 (3)	3 (3)	3 (3)	3 (3)	3 (3)	3 (3)
SH	1 (3)	1 (3)	1 (3)	1 (3)	1 (3)	3 (3)	3 (3)	1 (3)	1 (3)
PPgp	0 (2)	0 (2)	0 (2)	1 (3)	1 (3)	2 (2)	1 (3)	1 (3)	0 (2)

(c) Specific surface area ( $\text{m}^2 \text{kg}^{-1}$ )									
Grain shape	PP	DF	RG	FC	DH	MF	IF	SH	PPgp
SSA	40	30	20	25	4	7	2	4	20

Table B.1. Conversion of observed grain shape into the model grain morphology variables: (a) sphericity, (b) historic variable and (c) specific surface area. Snow shape abbreviations correspond to the international classification of seasonal snow on the ground [Fierz et al., 2009]. For the historic variable (b), the value in brackets is used when the observed layer is wet. Sphericity and historic variables were determined to be coherent with grain identification implemented in Crocus code [Vionnet et al., 2012]. Specific surface area ranges are determined the same way but Crocus having only three classes, relative value between grains in the same class are determined by measurements from Carmagnola, 2013 and Domine et al., 2007. This last table is more simple because of the lack of data and the difference in absolute values between measured and simulated specific surface area.

Secondary grain	PP	DF	RG	FC	DH	MF	IF	SH	PPgp
Main grain									
PP	100	150	150	100	100	180	180	100	120
DF	150	180	230	200	200	250	250	180	180
RG	200	230	300	250	250	350	450	200	200
FC	180	200	250	250	280	350	450	180	200
DH	180	200	250	280	300	350	450	180	200
MF	180	250	350	350	350	400	450	400	350
IF	180	250	450	450	450	450	450	450	450
SH	100	180	200	180	180	400	450	100	250
PPgp	120	180	200	200	200	350	450	250	250

Table B.2. Snow density ( $\text{kg}\cdot\text{m}^{-3}$ ) associated with grain shape, taking into account the main grain shape and the secondary one.

- 524 D'Amboise, C.J.L., Müller, K., Oxarango, L., Morin, S., Schuler, T.V., 2017. Implementation of a physically based water percolation routine in  
525 the crocus (v7) snowpack model. *Geoscientific Model Development Discussions* 2017, 1–32. doi:10.5194/gmd-2017-56.
- 526 Decharme, B., Boone, A., Delire, C., Noilhan, J., 2011. Local evaluation of the interaction between soil biosphere atmosphere soil multilayer  
527 diffusion scheme using four pedotransfer functions. *Journal of Geophysical Research: Atmospheres* 116. doi:10.1029/2011JD016002.
- 528 Domine, F., Morin, S., Brun, E., Lafaysse, M., Carmagnola, C., 2013. Seasonal evolution of snow permeability under equi-temperature and  
529 temperature-gradient conditions. *The Cryosphere* 7, 1915–1929. doi:10.5194/tc-7-1915-2013.
- 530 Domine, F., Taillandier, A.S., Simpson, W.R., 2007. A parameterization of the specific surface area of seasonal snow for field use and for models  
531 of snowpack evolution. *Journal of geophysical research* 112, F0231. doi:10.1029/2006JF000512.
- 532 Douville, H., Royer, J.F., Mahfouf, J.F., 1995. A new snow parameterization for the meteo-france climate model. *Climate Dynamics* 12, 21–35.
- 533 Durand, Y., Giraud, G., Brun, E., Mérindol, L., Martin, E., 1999. A computer-based system simulating snowpack structures as a tool for regional  
534 avalanche forecasting. *Journal of Glaciology* 45, 469–484. doi:10.1017/S002214300001337.
- 535 Durand, Y., Laternser, M., G.Giraud, P.Etchevers, B.Lesaffre, Mérindol, L., 2009. Reanalysis of 44 yr of climate in the french alps (1958–2002):  
536 Methodology, model validation, climatology, and trends for air temperature and precipitation. *Journal of applied meteorology and climatology*  
537 48, 429–449. doi:10.1175/2008JAMC1808.1.
- 538 Essery, R., Morin, S., Lejeune, Y., Ménard, C., 2013. A comparison of 1701 snow models using observations from an alpine site. *Advances in*  
539 *Water Resources* 55, 131–148. doi:10.1016/j.advwatres.2012.07.013.
- 540 Fierz, C., Armstrong, R., Durand, Y., Etchevers, P., Greene, E., McClung, D., Nishimura, K., Satyawali, P., Sokratov, S., 2009. The international  
541 classification for seasonal snow on the ground. *IHP-VII Technical Documents in Hydrology* 83.
- 542 Fierz, C., Gerber, F., Lehning, M., 2014. Comparison of modelled and measured point snow profiles: a tool for validating snow-cover models of  
543 the next generation?, in: *Proceedings of International Snow Science Workshop, Bandd*. pp. 825–826.
- 544 Giraud, G., Martin, E., Brun, E., Navarre, J.P., 2002. *Crocusmeprapc* software: a tool for local simulations of snow cover stratigraphy and  
545 avalanche risks. *International Snow Science Workshop*.
- 546 Hagenmuller, P., van Herwijnen, A., Pielmeier, C., Marshall, H.P., 2018. Evaluation of the snow penetrometer avatech sp2. *Cold Regions Science*  
547 *and Technology* 149, 83–94. doi:10.1016/j.coldregions.2018.02.006.
- 548 Hagenmuller, P., Pilloix, T., 2016. A new method for comparing and matching snow profiles, application for profiles measured by penetrometers.  
549 *Frontiers in Earth Science* 4, 1–13. doi:10.3389/feart.2016.00052.

- 550 Hagenmuller, P., Pilloix, T., Lejeune, Y., 2016. Inter-comparison of snow penetrometers (ramsonde, avatech sp2 and snowmi-cropen) in the  
551 framework of avalanche forecasting, in: International Snow Science Workshop, Breckenridge, Colorado, USA, pp. 32–38.
- 552 Harper, J., Bradford, J., 2003. Snow stratigraphy over a uniform depositional surface: spatial variability and measurement tools. *Cold Regions*  
553 *Science and Technology* 37, 289–298. doi:10.1016/S0165-232X(03)00071-5.
- 554 Helfricht, K., Hartl, L., Koch, R., Marty, C., Olefs, M., 2018. Obtaining sub-daily new snow density from automated measurements in high  
555 mountain regions. *Hydrology and Earth System Sciences* 22, 2655–2668. doi:10.5194/hess-22-2655-2018.
- 556 Helmert, J., Şensoy Şorman, A., Alvarado Montero, R., De Michele, C., de Rosnay, P., Dumont, M., Finger, D., Lange, M., Picard, G., Potopová,  
557 V., et al., 2018. Review of snow data assimilation methods for hydrological, land surface, meteorological and climate models: Results from a  
558 cost harnosnow survey. *Geosciences* 8, 489. doi:10.3390/geosciences8120489.
- 559 Jordan, R., 1991. A one-dimensional temperature model for a snow cover: Technical documentation for SNTHERM 89. Technical Report. Cold  
560 regions research and engineering lab, Hanover NH.
- 561 Krinner, G., Derksen, C., Essery, R., Flanner, M., Hagemann, S., Clark, M., Hall, A., Rott, H., Brutel-Vuilmet, C., Kim, H., Ménard, C.B.,  
562 Mudryk, L., Thackeray, C., Wang, L., Arduini, G., Balsamo, G., Bartlett, P., Boike, J., Boone, A., Chéruiy, F., Colin, J., Cuntz, M., Dai, Y.,  
563 Decharme, B., Derry, J., Ducharne, A., Dutra, E., Fang, X., Fierz, C., Ghattas, J., Gusev, Y., Haverd, V., Kontu, A., Lafaysse, M., Law, R.,  
564 Lawrence, D., Li, W., Marke, T., Marks, D., Ménégoz, M., Nasonova, O., Nitta, T., Niwano, M., Pomeroy, J., Raleigh, M.S., Schaedler, G.,  
565 Semenov, V., Smirnova, T.G., Stacke, T., Strasser, U., Svenson, S., Turkov, D., Wang, T., Wever, N., Yuan, H., Zhou, W., Zhu, D., 2018.  
566 Esm-snowmip: assessing snow models and quantifying snow-related climate feedbacks. *Geoscientific Model Development* 11, 5027–5049.  
567 doi:10.5194/gmd-11-5027-2018.
- 568 Lafaysse, M., Cluzet, B., Dumont, M., Lejeune, Y., Vionnet, V., Morin, S., 2017. A multiphysical ensemble system of numerical snow modelling.  
569 *The Cryosphere* 11, 1173–1198.
- 570 Lafaysse, M., Morin, S., Coléou, C., Vernay, M., Serca, D., Besson, F., Willemet, J.M., Giraud, G., Durand, Y., 2013. Towards a new chain of  
571 models for avalanche hazard forecasting in french mountain ranges, including low altitude mountains. *Proceedings of International snow science*  
572 *workshop Grenoble* .
- 573 Langeron, C., Dumont, M., Morin, S., Boone, A., Lafaysse, M., Metref, S., Cosme, E., Jonas, T., Winstral, A., Margulis, S.A., 2020. Toward snow  
574 estimation in mountains areas using modern data assimilation methods: A review. *Frontiers Submitted*.
- 575 Larue, F., Royer, A., De Sève, D., Roy, A., Picard, G., Vionnet, V., Cosme, E., 2018. Simulation and assimilation of passive microwave data  
576 using a snowpack model coupled to a calibrated radiative transfer model over northeastern canada. *Water Resources Research* 54, 4823–4848.  
577 doi:10.1029/2017WR022132.
- 578 Lehning, M., Bartelt, P., Brown, B., Fierz, C., Satyawali, P., 2002. A physical snowpack model for the swiss avalanche warning: Part ii. snow  
579 microstructure. *Cold regions science and technology* 35, 147–167.
- 580 Lehning, M., Fierz, C., Lundy, C., 2001. An objective snow profile comparison method and its application to snowpack. *Cold Regions Science and*  
581 *Technology* 33, 253–261. doi:10.1016/S0165-232X(01)00044-1.
- 582 Lejeune, Y., Dumont, M., Panel, J.M., Lafaysse, M., Lapalus, P., Le Gac, E., Lesaffre, B., Morin, S., 2019. 57 years (1960–2017) of snow and  
583 meteorological observations from a mid-altitude mountain site (col de porte, france, 1325 m of altitude). *Earth System Science Data* 11, 71–88.  
584 doi:10.5194/essd-11-71-2019.
- 585 Loth, B., Graf, H.F., 1998. Modeling the snow cover in climate studies: 1. long-term integrations under different climatic conditions using a  
586 multilayered snow-cover model. *Journal of Geophysical Research: Atmospheres* 103, 11313–11327. doi:10.1029/97JD01411.
- 587 Magnusson, J., Gustafsson, D., Hüsler, F., Jonas, T., 2014. Assimilation of point swe data into a distributed snow cover model comparing two  
588 contrasting methods. *Water Resources Research* 50, 7816–7835. doi:10.1002/2014WR015302.
- 589 Morin, S., Domine, F., Dufour, A., Lejeune, Y., Lesaffre, B., Willemet, J.M., Carmagnola, C., Jacobi, H.W., 2013. Measurements and modeling of  
590 the vertical profile of specific surface area of an alpine snowpack. *Advances in Water Resources* 55, 111–120. doi:10.1016/j.advwatres.  
591 2012.01.010.
- 592 Morin, S., Horton, S., Techel, F., Bavay, M., Coléou, C., Fierz, C., Gobiet, A., Hagenmuller, P., Lafaysse, M., Ližar, M., Mitterer, C., Monti, F.,

- 593 Müller, K., Olefs, M., Snook, J.S., van Herwijnen, A., Vionnet, V., 2019. Application of physical snowpack models in support of operational  
594 avalanche hazard forecasting: A status report on current implementations and prospects for the future. *Cold Regions Science and Technology* ,  
595 102910doi:https://doi.org/10.1016/j.coldregions.2019.102910.
- 596 Morin, S., Lejeune, Y., Lesaffre, B., Panel, J.M., Poncet, D., David, P., Sudul, M., 2012. An 18-yr long (1993–2011) snow and meteorological  
597 dataset from a mid-altitude mountain site (col de porte, france, 1325 m alt.) for driving and evaluating snowpack models. *Earth System Science*  
598 *Data* 4, 13–21. doi:10.5194/essdd-5-29-2012.
- 599 Pahaut, E., Giraud, G., 1995. Avalanche risk forecasting in france: results and prospects. *La Météorologie* .
- 600 Piazzzi, G., Thirel, G., Campo, L., Gabellani, S., 2018. A particle filter scheme for multivariate data assimilation into a point-scale snowpack model  
601 in an alpine environment. *The Cryosphere* 12, 2287–2306. doi:10.5194/tc-12-2287-2018.
- 602 Pielmeier, C., Schneebeli, M., 2003. Stratigraphy and changes in hardness of snow measured by hand, ramsonde and snow micro penetrometer: a  
603 comparison with planar sections. *Cold Regions Science and Technology* 37, 393–405.
- 604 Proksch, M., Rutter, N., Fierz, C., Schneebeli, M., 2016. Intercomparison of snow density measurements: bias, precision, and vertical resolution.  
605 *The Cryosphere* 10, 371–384. doi:10.5194/tc-10-371-2016.
- 606 Raleigh, M., Lundquist, J., Clark, M., 2015. Exploring the impact of forcing error characteristics on physically based snow simulations within a  
607 global sensitivity analysis framework. *Hydrology and Earth System Science* 19, 3153–3179. doi:10.5194/hess-19-3153-2015.
- 608 Revuelto, J., Lecourt, G., Lafaysse, M., Zin, I., Charrois, L., Vionnet, V., Dumont, M., Rabatel, A., Six, D., Condom, T., et al., 2018. Multi-  
609 criteria evaluation of snowpack simulations in complex alpine terrain using satellite and in situ observations. *Remote Sensing* 10, 1171.  
610 doi:10.3390/rs10081171.
- 611 Sakoe, H., Chiba, S., 1978. Dynamic programming algorithm optimization for spoken word recognition. *IEEE Transactions on Acoustics, Speech,*  
612 *and Signal Processing* 26, 43–49. doi:10.1109/TASSP.1978.1163055.
- 613 Schaller, C.F., Freitag, J., Kipfstuhl, S., Laepple, T., Steen-Larsen, H.C., Eisen, O., 2016. A representative density profile of the north greenland  
614 snowpack. *The Cryosphere* 10, 1991–2002. doi:10.5194/tc-10-1991-2016.
- 615 Schweizer, J., Bruce Jamieson, J., Schneebeli, M., 2003. Snow avalanche formation. *Reviews of Geophysics* 41.
- 616 Smyth, E.J., Raleigh, M.S., Small, E.E., 2019. Particle filter data assimilation of monthly snow depth observations improves estimation of snow  
617 density and swe. *Water Resources Research* 55, 1296–1311. doi:10.1029/2018WR023400.
- 618 Vionnet, V., Brun, E., Morin, S., Boone, A., Faroux, S., Moigne, P.L., Martin, E., Willemet, J.M., 2012. The detailed snowpack scheme crocus and  
619 its implementation in surfex v7.2. *Geoscientific model development* 5, 773–791. doi:10.5194/gmd-5-773-2012.
- 620 Vionnet, V., Guyomarc'h, G., Lafaysse, M., Naaim-Bouvet, F., Giraud, G., Deliot, Y., 2018. Operational implementation and evaluation of a  
621 blowing snow scheme for avalanche hazard forecasting. *Cold Regions Science and Technology* 147, 1–10. doi:10.1016/j.coldregions.  
622 2017.12.006.
- 623 Vionnet, V., Six, D., Auger, L., Dumont, M., Lafaysse, M., Quéno, L., Réveillet, M., Dombrowski-Etchevers, I., Thibert, E., Vincent, C., 2019.  
624 Sub-kilometer precipitation datasets for snowpack and glacier modeling in alpine terrain. *Frontiers in Earth Science* 7, 182. doi:10.3389/  
625 *feart*.2019.00182.
- 626 Wever, N., Fierz, C., Mitterer, C., Hirashima, H., Lehning, M., 2014. Solving richards equation for snow improves snowpack meltwater runoff  
627 estimations in detailed multi-layer snowpack model. *The Cryosphere* 8, 257.